



Evolutionary demography: the dynamic and broad intersection of ecology and evolution

Unexplained variability among spatial replicates in transient elasticity: implications for evolutionary ecology and management of invasive species

Carol C. Horvitz¹ · Julie S. Denslow² · Tracy Johnson¹ · Orou Gaoue^{4,5} · Amanda Uowolo³

Received: 22 June 2017 / Accepted: 12 April 2018 / Published online: 3 May 2018
© The Society of Population Ecology and Springer Japan KK, part of Springer Nature 2018

Abstract

Understanding actual and potential selection on traits of invasive species requires an assessment of the sources of variation in demographic rates. While some of this variation is assignable to environmental, biotic or historical factors, unexplained demographic variation also may play an important role. Even when sites and populations are chosen as replicates, the residual variation in demographic rates can lead to unexplained divergence of asymptotic and transient population dynamics. This kind of divergence could be important for understanding long- and short- term differences among populations of invasive species, but little is known about it. We investigated the demography of a small invasive tree *Psidium cattleianum* Sabine in the rainforest of Hawai‘i at four sites chosen for their ecological similarity. Specifically, we parameterized and analyzed integral projection models (IPM) to investigate projected variability among replicate populations in: (1) total population size and annual per capita population growth rate during the transient and asymptotic periods; (2) population structure initially and asymptotically; (3) three key parameters that characterize transient dynamics (the weighted distance of the structure at each time step from the asymptotic structure, the strength of the sub-dominant relative to the dominant dynamics, and inherent cyclicity in the subdominant); and (4) proportional sensitivity (elasticity) of population growth rates (both asymptotic and transient) to perturbations of various components of the life cycle. We found substantial variability among replicate populations in all these aspects of the dynamics. We discuss potential consequences of variability across ecologically similar sites for management and evolutionary ecology in the exotic range of invasive species.

Keywords Hawai‘i · Integral projection model · Invasive tree · *Psidium cattleianum* · Selection during transient dynamics

Electronic supplementary material The online version of this article (<https://doi.org/10.1007/s10144-018-0613-x>) contains supplementary material, which is available to authorized users.

✉ Carol C. Horvitz
carolhorvitz@miami.edu

- ¹ Department of Biology, Institute of Theoretical and Mathematical Ecology, University of Miami, PO Box 249118, Coral Gables, FL 33124, USA
- ² Department of Ecology and Evolutionary Biology, Tulane University, New Orleans, LA 70118, USA
- ³ USDA Forest Service, Institute of Pacific Islands Forestry, Volcano, HI 96785, USA
- ⁴ Department of Botany, University of Hawai‘i at Manoa, 3190 Maile Way, St. John 101, Office 405C, Honolulu, HI 96822, USA
- ⁵ Universite de Parakou, BP 123, Parakou, Benin

Introduction

Demography of invasive species may exhibit spatial variation due to known environmental factors, including abiotic factors (e.g., moisture, temperature), biotic factors (e.g., the presence/absence of enemies and mutualists), or historical factors (e.g., time since introduction, source of introduction). However, even when populations are similar in all known respects, variation in demographic rates may remain. Such divergence among replicates could be important because they translate mathematically to short- and long- term differences in population dynamics and to differences in selection on traits of the species, but little is known about it. For example, consider whether management protocols, e.g., introduction of a biological control agent, will be equally

successful across similar sites. Transient dynamics differ from long-term asymptotic dynamics most when the initial stage structure is far from the asymptotic stage structure and when the non-dominant dynamics are strong relative to the dominant (Caswell 2001, 2007; Haridas and Tuljapurkar 2007; Iles et al. 2016). We investigate transient elasticities, defined as proportional sensitivities of time-step-specific per capita population growth rates $\lambda(t)$ during the non-asymptotic phase of population growth (Haridas and Tuljapurkar 2007; Maron et al. 2010) (see Caswell (2007) for a focus on sensitivity of the cumulative growth rate [from time 0 to time t] rather than the time-step specific growth rate [from time t to time $t + 1$]).

Transient dynamics refer to changes in population size and structure before structured populations have reached the *stable stage distribution*. The fundamental point for our application is that the importance of particular stages and transitions to annual population growth may vary over the transient phase. Thus, any interaction, management protocol or trait that influences a particular stage may wax and wane in its influence on population growth. Since methods for performing a sensitivity analysis of non-asymptotic annual population growth rate are relatively new and developing rapidly (Fox and Gurevitch 2000; Koons et al. 2005; Caswell 2007; Haridas and Tuljapurkar 2007; Townley et al. 2007; Townley and Hodgson 2008; Stott et al. 2010; Gaoue 2016; Iles et al. 2016), we clarify how we apply these methods and briefly recapitulate some of the important parameters underlying transient dynamics, taking into account the distance an initial stage structure is from the stable stage distribution (as in Haridas and Tuljapurkar 2007). A distinct, but related, approach to transient analysis that does not take into account initial structure is presented by Stott et al. (2010) who emphasize situations where a population that has been at a stable equilibrium is suddenly perturbed. In that context, the concern is the magnitude of the envelope within which the transient dynamics may occur and how far away they will get from the stable after the perturbation. In the current context we are interested in populations not yet at a stable stage distribution. The start can be considered some particular initial time 0 and the dynamics at each subsequent time step are of interest. In other words, our approach emphasizes how long it will take to get to the stable stage distribution from some known starting point, while Stott et al.'s (2010) approach emphasizes how far away the population will get from the stable stage distribution after a perturbation.

We investigated the demography of a small invasive tree in the rainforest of Hawai'i in four populations chosen for their ecological similarity as replicates. Specifically, we asked the following: how much residual spatial variability is there in: (1) total population size and annual per capita population growth rate during the transient and asymptotic periods; (2) population structure initially and asymptotically;

(3) three key parameters that characterize transient dynamics (the weighted distance of the structure at each time step from the asymptotic structure, the strength of the sub-dominant relative to the dominant dynamics, and inherent cyclicity in the subdominant); and (4) proportional sensitivity (elasticity) of population growth rates (both asymptotic and transient) to perturbations of various components of the life cycle? We use elasticity analysis to explore differences in stage-specific effects among replicate populations.

Methods

We parameterized integral projection models (IPM) of plant population dynamics at several sites of the invasive pest plant *Psidium cattleianum* Sabine (Myrtaceae) (Strawberry guava) in Hawai'i. We used detailed, demographic data collected over multiple years at each site. The native range of strawberry guava is the Atlantic coastal forest of Brazil; its non-native range includes islands in the tropical Pacific and Indian Oceans. Similar to other invasive shade-tolerant woody species (Horvitz et al. 1998), strawberry guava is able to establish in intact forest where it dominates the understory and lower canopy. In Hawai'i, this invader changes rain forest structure (Asner et al. 2009), altering ecosystem processes (Takahashi et al. 2011) and reducing suitable habitat for native species (Paul Banko, personal communication). Also, large populations of insect pests of soft agriculturally important fruits such as papaya are supported by decaying strawberry guava fruit presenting a formidable challenge to agricultural production. Our analyses provide a quantitative framework of how management protocols (like the introduction of a bio-control agent) could impact population dynamics in the short- and long-term differently among replicate populations. For example, in its native Brazil, strawberry guava sometimes experiences high levels of infestation by a native scale insect *Tectococcus ovatus*, Hempel (Homoptera: Eriococcidae) which has been proposed as a bio-control (Vitorino et al. 2000). Strawberry guava has been in Hawai'i without pests since 1825 (State of Hawai'i, Department of Agriculture 2011).

We studied demography of *P. cattleianum* at four similar sites on Hawai'i Island, within the Kahauale'a Natural Area Reserve (19°26'N, 155°10'W) (hereafter Kahauale'a), the Pu'u Maka'ala Natural Area Reserve (19°34'N, 155°12'W) (hereafter Maka'ala), the 'Ōla'a Forest Reserve (19°27'N, 155°11'W) (hereafter 'Ōla'a), and the Upper Waiākea Forest Reserve (19°35'N, 155°12'W) (hereafter Waiākea). Distances between study sites ranged from 2 to 17 km (mean = 10.8 km). The sites were chosen for their similarity with respect to climate, elevation, substrate and degree of invasion by *P. cattleianum*, rather than for any *a priori* distinction among them. All sites are on windward Hawai'i

Island at approximately 900 m elevation. Estimated annual rainfall is 3000–4000 mm at ‘Ōla‘a and Kahauale‘a and 4000–5000 mm at Waiākea and Maka‘ala (Giambelluca et al. 1986). Mean annual temperature is 17–17.5 °C for the elevation range of the four study sites (Giambelluca and Schroeder 1998). They are all on relatively young tholeiitic basalt lava flows that formed 200–1500 years BP (Wolfe and Morris 1996). The forests are classified as native lowland wet forests with an ‘ōhi‘a (*Metrosideros polymorpha* Gaud.) lowland wet forest community type (Gagne and Cuddihy 1999).

At each site, large study plots (50×50 m at all sites except ‘Ōla‘a where the dimension was 50×30 m) were established in 2005. The populations in the plots were sub-sampled at different scales to obtain data on individuals of different sizes. For stems with enough height and girth to reach the threshold diameter of 0.5 cm at 1.3 m above the ground, size was defined by DBH [diameter at breast height (1.3 m)]. Individuals were marked with numbered tags and censused for size and survival annually. New recruits were tagged when they appeared at the annual census. In this paper we analyze data on these individuals from 2005 to 2011, for a cumulative number of 21,846 observations of individual annual fates (Table 1).

For smaller stems (DBH < 0.5 cm), 40 quadrats (each 0.5×0.5 m) were established at each site in 2009. In these quadrats, plant size was defined by height class (< 10 cm, between 10 and 100 cm, or > 100 cm) and stem origin was defined by whether a stem was clearly arising vegetatively from another individual or not. Those not arising as vegetative sprouts were assumed to have recruited from seeds. Individuals were tagged by size class and stem origin. The number in each size×origin category in each quadrat was recorded annually, as well as counts of how many individuals of each size×origin category changed size or died. New recruits were counted at annual censuses. In this paper we analyze data from these quadrats from 2009 to 2013, for a cumulative number of 1858 observations of individual annual fates (Table 1). Previous work established that there is no seed bank for strawberry guava (Uowolo and Denslow

2008), so the current study did not address seed dormancy either empirically or in the model.

The model of population dynamics

To study population dynamics in discrete time, we parameterized an integral projection model (IPM),

$$n(y, t + 1) = \int K(y, x) n(x, t), \quad (1)$$

where demography depends upon size, the population at a given time t is represented by a numerical density function $n(x, t)$ across all possible sizes and the kernel $K(y, x)$ is a surface that quantifies how individuals of size x at time t contribute to or become individuals of size y at time $t + 1$. The time step of our model is 1 year. To capture the dynamics of both large and small stems, we created a kernel that was comprised of two domains, a discrete domain for the small stems (DBH < 0.5 cm) and a continuous domain for the larger stems (DBH ≥ 0.5 cm). Three discrete sizes for the small stems were height classes, and the continuous size variable for large stems was DBH (diameter at breast height). This model is a density-independent model.

We parameterized the dynamics within and between these domains (Fig. 1) for populations at each of the four study sites. To parameterize the discrete domain component of the model, we estimated maximum likelihoods of annual survival and transition probabilities from counts in contingency tables, where observations are classified by survival or death from 1 year to the next and cross-classified by current and future sizes for individuals that survive (Caswell 2001). In the discrete domain, rates of survival and size transitioning depended upon whether stems originated vegetatively or from sexually produced seeds as well as on their size. To parameterize the continuous domain component of the model, we used standard statistical analysis to quantitatively relate the mean and variance of demographic fates to one (or more) continuous predictor variable(s). For example, logistic regression quantitatively predicts the probability of survival for any size. Similarly,

Table 1 Stratified sampling regime for stems of different sizes at four study sites

Stem size	Size of each sample plot [m ²]	Number of sample plots total	Number of sample plots per site	Range of years	Initial number of stems	Cumulative number of observations of annual fates	For which domain of model?
<0.5 cm DBH	0.25	160	40	2009–2013	374	1858	Discrete
>0.5 cm DBH							
DBH < 2 cm	25	27	5–11	2005–2011			
DBH ≥ 2 cm	25	360	60–100	2005–2011			
Total					1481	21,846	Continuous

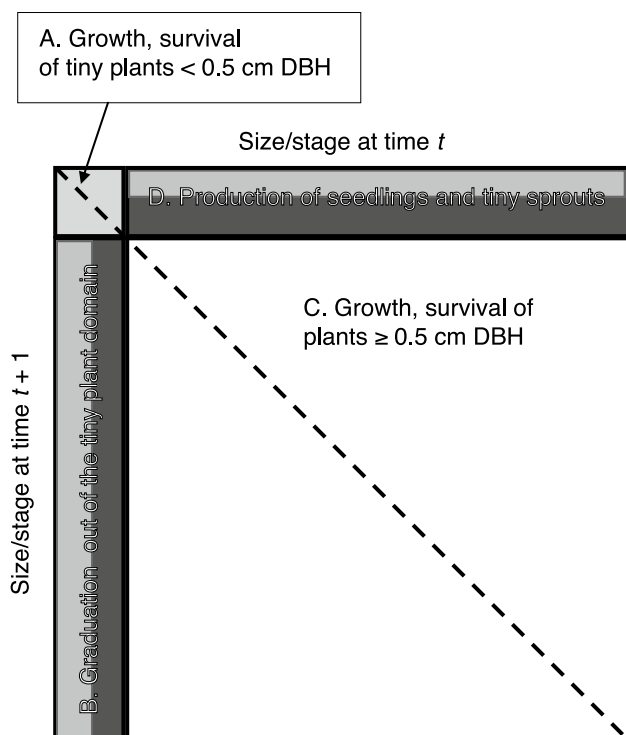


Fig. 1 Schematic diagram of our 206×206 population projection matrix model comprised of four blocks: **A** regression, growth and survival of plants < 0.5 cm DBH are modeled in the upper left 6×6 square, where the 6 categories are 3 height classes \times 2 stem origin classes (seedlings in columns 1–3 and sprouts in columns 4–6); **B** “graduation” out of this block into specific size classes ≥ 0.5 cm DBH are modeled in the 200×6 rectangle directly under A; **C** regression, growth and survival of plants ≥ 0.5 cm DBH are modeled in the lower right 200×200 square, where the 200 categories are intervals of equal width of DBH; and **D** Production of seedlings (rows 1–3) and sprouts (rows 4–6) by plants ≥ 0.5 cm DBH are modeled in the 6×200 rectangle directly above C. Blocks A and B were parameterized by maximum likelihood estimation using counts of plants in discrete categories. Blocks C and D were parameterized by discretizing a continuous integral projection surface. The dotted line indicates the diagonal. Along it, the matrix entries indicate that over one time interval, plants of a given size become or contribute to the number of plants of that same size; above it plants of a given size become or contribute to the number of plants of smaller size; and below it plants of a given size become or contribute to the number of plants of larger size

linear regression quantitatively predicts size in the future from any current size for survivors. Regression analyses and all the tools available from statistics are at the heart of parameterizing the integral surface of an IPM (Easterling et al. 2000; Ellner and Rees 2006). In both domains, individuals who survive could remain the same size, become larger or smaller and could reproduce during the annual time step. After the model has been fully parameterized, the continuous variable, in practice, is discretized into intervals of equal width and the integral kernel surface is approximated by a high dimensional matrix (Fig. 1). Then,

all the tools of matrix analysis are available to elucidate population dynamics, both transient and asymptotic.

In this paper we parameterized a single IPM for each study population, pooling observations across years, but not sites. The years of observations included in this analysis were 2005–2011 for the large stems and 2009–2013 for the small stems. Statistical analyses and parameterization of the underlying models are not the main subject of this paper, but we provide the 54 parameters that we estimated for each site in an electronic supplement (Electronic Supplementary Material (ESM) S1). At the heart of our investigation is a 206×206 matrix for each population. The continuous domain was discretized into 200 size categories and the discrete domain included 6 size \times stem-origin categories (Fig. 1). To choose the number of categories in the continuous domain, we assayed a series of mesh sizes and found that λ 's stabilized around 200 mesh points. Our study species is a small tree with a maximum observed size of 18.9 cm. Zuidema et al. (2010) recommend that intervals used for tree IPM's not be wider than 1 cm. Each interval of our model corresponded to a width of 0.093 cm, clearly not exceeding the recommendation. Each of our 200 stages was named by the midpoint of the DBH interval that it represented. To construct stage structure distributions for individual years, we scaled up stem densities of particular sizes at a particular point in time to “individuals per hectare.” In this paper we use the 2009 data, the first year for which we had data for both domains, to construct the population structure that we consider to be the initial ($t = 0$) structure.

Population projection: transient and asymptotic dynamics

Once we have discretized the kernel of the IPM, we can then proceed with analysis of the corresponding population projection matrix model, which is often written as a difference equation that projects a population from one time to the next,

$$\mathbf{n}(t + 1) = \mathbf{A} \mathbf{n}(t). \quad (2)$$

Here we are more interested in expressing the population dynamics as a trajectory over time, starting from an initial state,

$$\mathbf{n}(t) = \mathbf{A}^t \mathbf{n}(0) \quad (3)$$

where $\mathbf{n}(t)$ is the vector of number of individuals at some time t in each of several discrete categories, \mathbf{A} is the matrix comprised of entries a_{ij} that represent how individuals in category j contribute to or become individuals in category i after a single time step, the matrix is raised to the t th power by matrix multiplication for its cumulative action after t time steps, and $\mathbf{n}(0)$ is the vector of the number of individuals in each category at a specific initial time ($t = 0$). This process can be thought of as having a transient phase during which

dynamics are influenced notably by initial conditions matter and an asymptotic phase during which dynamics are independent of initial conditions.

While asymptotic dynamics are appropriate for studying long term properties like the *stable stage distribution* (given by the dominant right eigenvector \mathbf{u}_{dom} of the matrix) and the eventual per capita rate of population increase (given by the dominant eigenvalue λ_{dom} of the matrix) (see “Appendix”), there are many issues that require an understanding of what goes on in the short term, before the population attains the *stable stage distribution*. During the transient phase, the dynamics are not independent of the initial population structure and the per capita rate at which the population grows is not constant, it may rise and fall. Similarly, the structure of the population is also not constant; it may be primarily made up of reproductives at one time and of juveniles at another, for example. Not only does the annual population growth rate, $\lambda(t) = N(t+1)/N(t)$, itself change with time, but so does its sensitivity; it may be more sensitive to perturbations of juvenile survival at one time and more sensitive to adult survival at another, for example. Such differences could be crucial in attempting to manage population growth of an invasive species by introducing a biocontrol agent that targets particular life stages or events during the life cycle (Maron et al. 2010).

Here, to gain insight into when/where bio-controls would have greatest effects during the near term, we performed transient analysis and we calculated transient elasticities (proportional sensitivities) of the annual transient growth rates $\lambda(t)$ following the method of Haridas and Tuljapurkar (2007) (also see Maron et al. 2010). For the transient analysis we focused on three key quantities:

$\alpha(t)$ is the scalar product of the population structure at time t with the normalized dominant left eigenvector \mathbf{v}_{dom} (see “Appendix”). It measures the distance of the population structure at each point in time from the asymptotic population structure \mathbf{u}_{dom} . When $\alpha(t) > 1$, there is an excess of individuals in stages with high reproductive value, but when $\alpha(t) < 1$, there is an excess of individuals in stages with low reproductive value relative to the asymptotic. $\alpha(0)$ equals Keyfitz’s (1968) well-known quantity population momentum (Haridas and Tuljapurkar 2007).

ρ is the damping ratio, $|\lambda_{subdom}|/\lambda_{dom}$. The subdominant eigenvalue is the one that is the second largest in magnitude. This ratio measures the degree of dominance or relative strength of the dominant. When $\rho \ll 1$, the dominant takes over quickly, but when ρ is close to 1, the dominant is not very dominant and the transients may be important for a longer period.

μ is the number of time steps it takes for a complex subdominant eigenvalue to complete one oscillation in the

complex plane. It measures periodicity inherent in the subdominant eigenvalue and suggests oscillations of population structure during the transient period.

A great deal of insight into the transient dynamics can be gained from these few parameters and others that can be calculated from the properties of the matrix.

Transient elasticity measures how a proportional tiny perturbation in a matrix element influences $\lambda(t)$. Unlike asymptotic elasticity it can be negative or positive. Haridas and Tuljapurkar (2007) show that transient elasticity can be decomposed into two additive components. They point out that a perturbation to an element of matrix \mathbf{A} results simultaneously in both a *perturbed matrix* $\mathbf{A} + \mathbf{C}$ (where \mathbf{C} is a matrix of zeros everywhere except for the particular rate which is being perturbed), and a *perturbed stable stage distribution*, which is the dominant right eigenvector of the *perturbed matrix*. The perturbation in the population growth rate is the result of both of these. Their respective effects can be separately calculated and then combined. Any given stage distribution is a certain distance from the *stable stage distribution* of the original matrix, and it is a different distance from the *stable stage distribution of the perturbed matrix*. Recall from above that $\alpha(t)$ is a scalar that measures the distance of stage structure at time t from the *stable stage distribution*. Note that the perturbed matrix will produce a somewhat different sequence of stage distributions over time than the unperturbed matrix produces (even when starting from the same initial stage distribution). We could track these differences in projected stage structure over time. Let the sequences be comprised of vectors of stage structures at each time t , $\mathbf{y}(t)$ for the unperturbed matrix and a vector $\hat{\mathbf{y}}(t)$ for the perturbed matrix, and then the difference between them at any given time would be $\mathbf{w}(t) = \hat{\mathbf{y}}(t) - \mathbf{y}(t)$. As pointed out by Haridas and Tuljapurkar (2007), as t becomes large, $\mathbf{w}(t)$ converges on the difference between the *stable stage distribution* of the perturbed matrix and the *stable stage distribution* of the original matrix. The perturbed population’s growth rate differs from that of the original population both because vital rates have changed and because population structure changes.

Obtaining transient elasticities involves thinking about a full set of such time series (structures, growth rates, and distances from *stable stage distribution* for both original and perturbed matrices as well as differences in projected structures between original and perturbed matrices) for *each given* matrix element. Thus, for example, a 3×3 matrix with nine matrix elements would have nine sets of such time series. At its heart, the analysis calculates the component due to the perturbation of matrix elements ($e_{1,ij}(t)$), the component due to the perturbation of structure ($e_{2,ij}(t)$) and their summation ($e_{ij}(t)$) at each time step for each matrix element as in Haridas and Tuljapurkar (2007). Here, in our results,

we focus on the total $e_{ij}(t)$ for each matrix element rather than the components. For details on how to use the dynamic properties of the matrix and the distance of the initial population from the *stable stage distribution* to calculate these components, see Haridas and Tuljapurkar (2007). Haridas kindly provided MATLAB code to us previously; our modified version of this code is available upon request.

Summarizing transient elasticity by life-history block

Our population matrices are 206×206 (Fig. 1). For each time step we have a transient elasticity matrix of the same dimension 206×206 . Rather than present a 20-time-step series of large matrices at each of 4 sites, we present broad patterns. To that end, we focus on sums of $e(t)$'s in different regions of the matrix. We consider the matrix to be divided into eight life history blocks. First we separate the columns for stems with $DBH < 0.5$ cm (columns 1–6) (Fig. 1a, b) from the columns for stems with $DBH \geq 0.5$ cm (columns 7–206) (Fig. 1c, d). For stems with $DBH < 0.5$ cm, we identify four life history blocks in the first six columns, noting that the top six rows form a square matrix of within-domain fates (Fig. 1a). (1) The first block is found above the diagonal of this matrix (“regression plus”) where matrix entries represent regression to smaller size classes plus some within-domain recruitment. (2) The second block is found along the diagonal and below it (“growth plus”) where matrix elements represent stasis plus growth plus some within-domain recruitment. (3) The third block is found in the first three columns of the 200 rows below this square where matrix elements represent the probability that small stems that originated from seeds grow sufficiently to attain $DBH \geq 0.5$ cm, thereby leaving the domain of small plants and entering particular size categories of the other domain (“graduation: sexual”) (Fig. 1b). (4) The fourth block is found in columns 4–6 of the 200 rows below the square where matrix elements represent the probability that small stems that originated vegetatively grow sufficiently to attain $DBH \geq 0.5$ cm, thereby leaving the domain of small plants and entering particular size categories of the other domain (“graduation: vegetative”) (Fig. 1b).

Similarly, for stems with $DBH \geq 0.5$ cm, we identify four life history blocks in the 200 columns that range from column 7 to 206, noting that within these, the bottom 200 rows form a square matrix of within-domain fates (Fig. 1c). (1) The first block is found above the diagonal of this matrix (“regression”) where matrix entries represent regression to smaller size classes. (2) The second block is found along the diagonal and below it (“growth”) where matrix elements represent stasis plus growth. (3) The third block, 200 columns wide, is found in the top three rows (rows 1–3) that are above this square where matrix elements represent

the number of sexually produced offspring (individuals with $DBH < 0.5$ cm belonging to each of the three discrete height classes) made per capita for each of the 200 size categories (“reproduction: sexual”) (Fig. 1d). (4) The fourth block, 200 columns wide, is found in next three rows (rows 4–6) above the square where matrix elements represent the number of vegetatively produced offspring (individuals with $DBH < 0.5$ cm belonging to each of the three discrete height classes) made per capita for each of the 200 size categories (“reproduction: vegetative”) (Fig. 1d).

Altogether then, we consider 8 life history blocks. To address broad issues, we present and compare the summed elasticities for these blocks.

Results

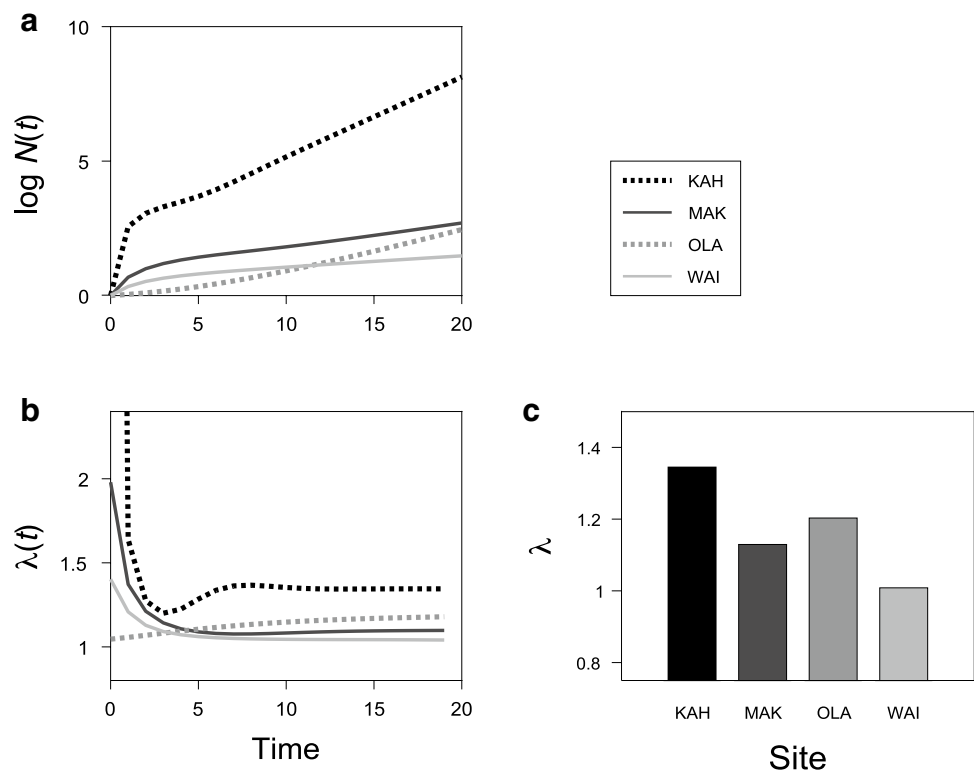
Population growth rates

There were surprising differences among the populations in both transient and asymptotic dynamics. Simply projecting the populations forward through time provided the trajectories of total population size $\log N(t)$ (Fig. 2a) and per-capita population growth rates at each time step $\lambda(t)$ (Fig. 2b). It is evident that the population at Kahauale‘a is growing considerably more rapidly than the populations at the other three sites throughout the transient period as well as asymptotically (Fig. 2). Because it starts with extremely rapid growth, $\lambda(1) = 13.0$ (off the chart, literally), the population at Kahauale‘a experiences the most dramatic drop off. In contrast the population at ‘Öla‘a is growing more slowly than any of the others during the first few years, $\lambda(1) = 1.05$, but it gradually increases in growth rate while populations at Maka‘ala and Waiākea both slow down, and ultimately, ‘Öla‘a attains the second highest growth rate (Fig. 2b, c). Asymptotically, population size at Waiākea is projected to nearly stabilize ($\lambda_{dom} = 1.01$), while at the other three sites, populations are projected to continue to increase by substantial proportions every year, ($\lambda_{dom} > 1.34, 1.13, \text{ and } 1.20$, respectively) (Fig. 2c).

Initial and asymptotic stage structure

Overall structure in 2009 (Fig. 3a) was similar among the populations (Fig. 3a), while asymptotically it differed substantially among the populations (Fig. 3b). For each of the four populations, initial structure differed rather dramatically from asymptotic structure. Also, initially, the percentage of the population that were small individuals ($DBH < 0.5$ cm) originating from seed was similar across the sites (14, 18, 20 and 44%), while asymptotically there was an order of magnitude variation across the sites (96, 36, 0.8 and 96%). The asymptotic stage structures at both Kahauale‘a and Waiākea

Fig. 2 Initial and asymptotic population dynamics at four study sites, Kahauale‘a (KAH), Maka‘ala (MAK), ‘Ōla‘a (OLA) and Waiākea (WAI) for 20 years starting with an initial population as observed in 2009. **a** Projection of total population, $\log N(t)$. **b** Transient annual per capita population growth rate, $\lambda(t) = N(t+1)/N(t)$. Not shown is the extremely high growth rate at Kahauale‘a Natural Area Reserve at the first time step ($\lambda(1) = 13.0$). **c** Asymptotic population growth rate, λ_{dom}



were strongly dominated by seedlings (DBH < 0.5 cm), while at Maka‘ala and ‘Ōla‘a, they were dominated by small vegetatively produced individuals (DBH < 0.5 cm).

For stems with DBH ≥ 0.05 cm, we combined stage classes into three broad groups. The groups were: the smallest 50 (midpoints 0.54–5.1 cm), the next 50 (midpoints 5.19–9.75 cm) and the largest 100 (midpoints 9.84–19.04 cm) stage classes of the discretized continuous domain. Among these groups, the first clearly dominates strongly both initially (Fig. 3c) and asymptotically (Fig. 3d) in all four populations. Also, the largest stems represent the lowest proportion both initially and asymptotically. At Kahauale‘a individuals of this size were absent initially and even asymptotically they were projected to represent only 2.6×10^{-11} of the total individuals (effectively zero for finite populations). At Maka‘ala and at ‘Ōla‘a, they initially comprised 6.3×10^{-4} and 6.5×10^{-4} of the population, respectively, both declining by several orders of magnitude asymptotically. Only at Waiākea do large individuals represent a comparatively large proportion of both the initial (3.0×10^{-3}) and asymptotic (1.2×10^{-3}) populations (still barely visible in Fig. 3c, d).

Transient dynamics in stage structure

Visualizing changes over 20 time steps in all 206 stages is not practical, so we view transient changes in stage structure by focusing on the 20 smallest stages (ESM S2) and the 10

largest stages (ESM S3). We use a log scale because parallel lines indicate stable, asymptotic structure, while lines that are not parallel indicate that stages are not increasing at the same rate and are not at the asymptotic structure. Among the 20 smallest sizes, the very small plants (DBH < 0.5 cm) increased most rapidly at first (except for the population at Waiākea), while the somewhat larger ones (DBH ≥ 0.5 cm) decreased at first, but then slowly increased (ESM S2). The relative abundances of many stages stabilized between $t = 10$ and $t = 20$. The 10 largest size classes were extremely low in abundance or entirely absent early on (except for at Waiākea), increasing by many orders of magnitude by the 20th time step (ESM S3).

Asymptotic reproductive value

Reproductive value vectors for all 206 stages (ESM S4) and for the 20 smallest stages (ESM S5) were generally similar across the four populations, but with notable variation in details. The shapes, not the numerical values on the y-axes, are of interest. The smallest stages had low reproductive value. Reproductive value for stems ≥ 0.5 cm DBH increased with size, sharply at Waiākea (ESM S4). The very small plants (DBH < 0.5 cm) had higher reproductive value at Maka‘ala than they did at other populations (ESM S4). Small stems originating vegetatively had higher reproductive value than small stems arising from seed. Reproductive value increased with height class of small stems (ESM S5).

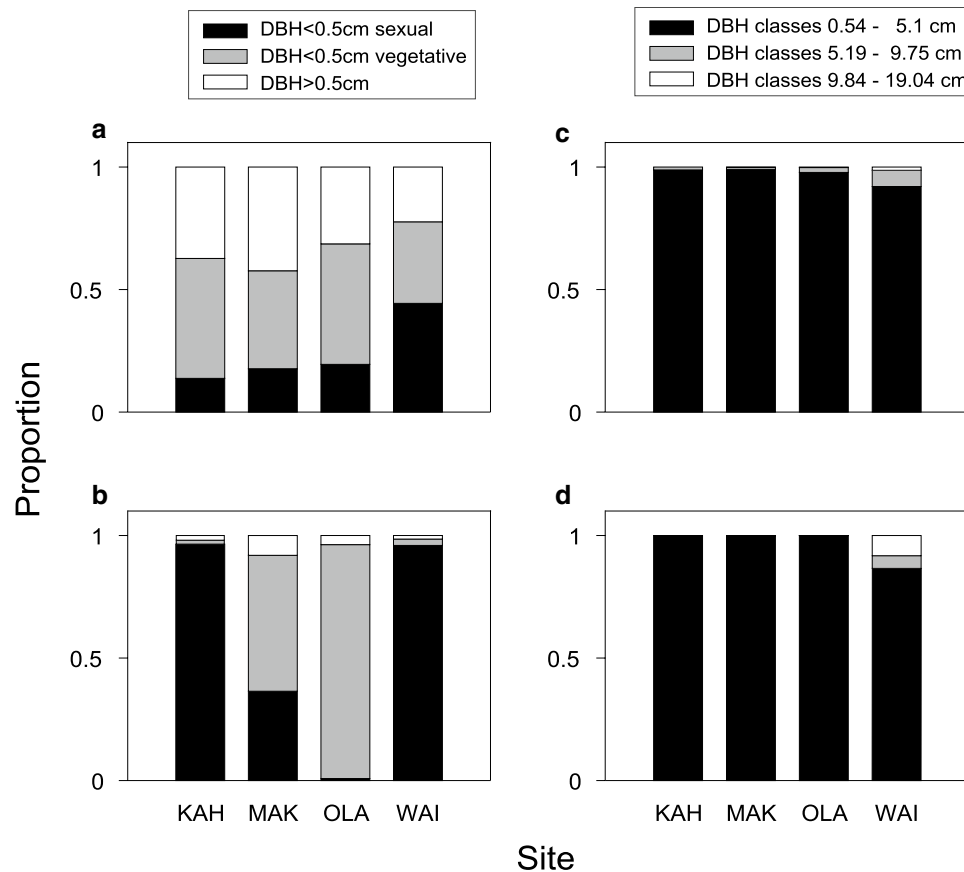


Fig. 3 Initial and asymptotic stage structure at four study sites, Kahauale‘a (KAH), Maka‘ala (MAK), ‘Ōla‘a (OLA) and Waiākea (WAI) starting with an initial population as observed in 2009. **a** Proportion of total *initial* population classified by domain, small stems (DBH < 0.5 cm) and large stems (DBH ≥ 0.5 cm); where small stems are further broken down into whether they originated sexually or vegetatively. **b** Proportion of total *asymptotic* population classified by domain, small stems (DBH < 0.5 cm) and large stems

(DBH ≥ 0.5 cm); with small stems further broken down into whether they originated sexually or vegetatively. **c** Proportion of large stems (DBH > 0.5 cm) in the *initial* population in the first 50 DBH classes, the next 50 DBH classes or the final 100 DBH classes, specified by the ranges of the midpoints of each class. **d** Proportion of large stems (DBH > 0.5 cm) in the *asymptotic* population in the first 50 DBH classes, the next 50 DBH classes or the final 100 DBH classes, specified by the ranges of the midpoints of each class

The pattern of reproductive values of stages 7–20 varied among the populations (ESM S5).

Key parameters of the transient dynamics: $\alpha(t)$, ρ , and μ

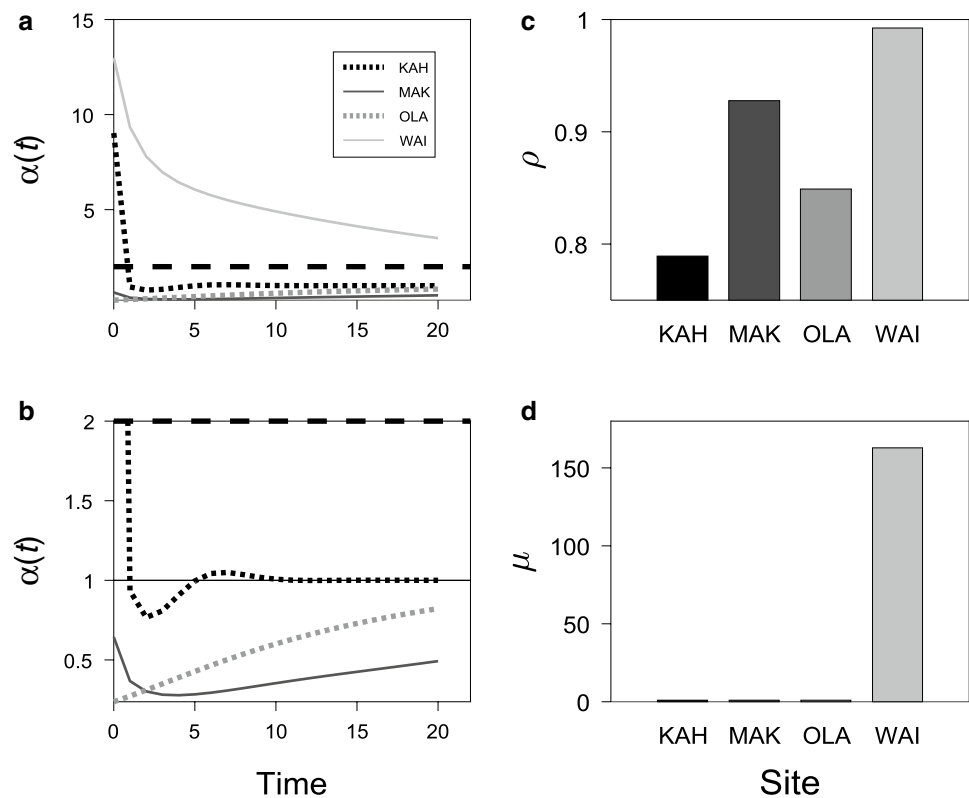
Parameters of the transient dynamics $\alpha(t)$ and ρ varied substantially across the populations (Fig. 4a, c). Only one site’s population, Waiākea, had a matrix with a complex subdominant eigenvalue, so it was the only one for which μ was defined (Fig. 4d).

The trajectory of weighted distances $\alpha(t)$ (Fig. 4a, b) of each population resembled the trajectory of population growth rates $\lambda(t)$ of each population (Fig. 2b). At Kahauale‘a, $\alpha(t)$ started very high, dropped rapidly, then exhibited shallow oscillations, and became approximately 1 by the 20th time step. At Waiākea, $\alpha(t)$ started even higher and gradually declined, but was still rather far from 1 by the

20th time step (Fig. 4a). At both Maka‘ala and at ‘Ōla‘a, $\alpha(t)$ started rather low, but their trajectories differed (Fig. 4b). The two sites with populations that were closest to attaining the stable stage distribution by the 20th time step are Kahauale‘a and ‘Ōla‘a. These are also the two sites where $\lambda(20)$ was the closest to the asymptotic population growth rate.

Of special interest is $\alpha(0)$, a measure of distance between the *initial* population and the *stable stage distribution*. It is a measure that includes a weighting by reproductive value. Recall that both initial and stable stage distributions varied among the populations (Fig. 3) as did the trajectories of stage structure during the transient period (ESM S2 and S3). Initially populations at Waiākea and Kahauale‘a had excess individuals in stages with relatively high reproductive value, $\alpha(0) > 1$, while initially populations at ‘Ōla‘a and at Maka‘ala had excess individuals in stages with relatively low reproductive value, $\alpha(0) < 1$. It is not possible to attribute

Fig. 4 Three key parameters of transient analysis at four study sites, Kahauale‘a (KAH), Maka‘ala (MAK), ‘Ōla‘a (OLA) and Waiākea (WAI). **a** $\alpha(t)$ measures the distance of the population structure at each point in time from the asymptotic population structure; note that when a population is at the *stable stage distribution*, $\alpha=1$. The dashed line does not indicate this threshold but rather it shows which portion of the plot will be expanded to view details. **b** Detail of (a), blown up to see the relative positions of the lines near the threshold; **c** ρ , the damping ratio; **d** μ , the number of time steps it takes for the subdominant eigenvalue to complete one cycle in the complex plane; the only site with a complex subdominant eigenvalue was the Waiākea (WAI)



these excesses to the effects of a single stage. First, although reproductive values generally increased with plant size in all the populations, the increase was not entirely monotonic and the pattern differed among the populations (ESM S4 and S5). In particular, the reproductive value vector for the population at Waiākea had a rather sharp increase starting at DBH approximately 1.5 cm, with a rather broad plateau over a wide range of sizes (ESM S4d). It contrasted with the other sites, where the largest stems had high reproductive value (ESM S5a,b and c). Second, the reproductive value of small stems that originated vegetatively was generally higher than that of comparably-sized stems that originated from seeds (ESM S5). Third, the extent to which reproductive value increased or decreased when individuals crossed over from the small domain to the large domain varied with site (ESM S5).

The ratio of the sub-dominant over the dominant eigenvalues, ρ , ranged from 0.79 (at Kahauale‘a) to 0.99 (at Waiākea) (Fig. 4c). By this measure we expect transient dynamics to be quite important at Waiākea, since the sub-dominant is nearly co-equal to the dominant eigenvalue. For example we might expect more notable oscillations in population growth rate and stage structure at this site than at others, but they are not apparent in the results. Further insight into the nature of the subdominant complex eigenvalue for this population is revealed by the parameter μ . Its value is around 150. That indicates a very small angle in

the complex plane, which means it would take 150 years to make a complete oscillation. These are very slow oscillations, and not much cyclicity will be revealed by a 20-time step projection. Nonetheless, the population at Waiākea was in fact farther from its asymptotic value at the 20th time step than any other, consistent with relatively more influence of transients at this site than at the other sites.

Asymptotic and transient elasticities

In three of the four study populations, asymptotic population growth was more sensitive to proportional perturbations of demographic rates affecting stems with $\text{DBH} < 0.5$ cm, than it was to perturbations of rates affecting plants with $\text{DBH} \geq 0.5$ cm. In fact for the population at ‘Ōla‘a, > 99% of the elasticity came from stems in the small domain. Only at Waiākea, was asymptotic population growth rate more sensitive to perturbations of demographic rates affecting plants with $\text{DBH} \geq 0.5$ cm (compare Fig. 5a, b). In both domains, at all sites, the biggest contributor to elasticity came from growth. Perturbation of growth parameters would have a large impact on asymptotic population dynamics. Asymptotic growth rates were much less sensitive to perturbations of other kinds of rates (regression, reproduction and graduation from small to large domain). One exception to this overall pattern was at Kahauale‘a, where production of offspring through seeds and graduation of small stems that originated

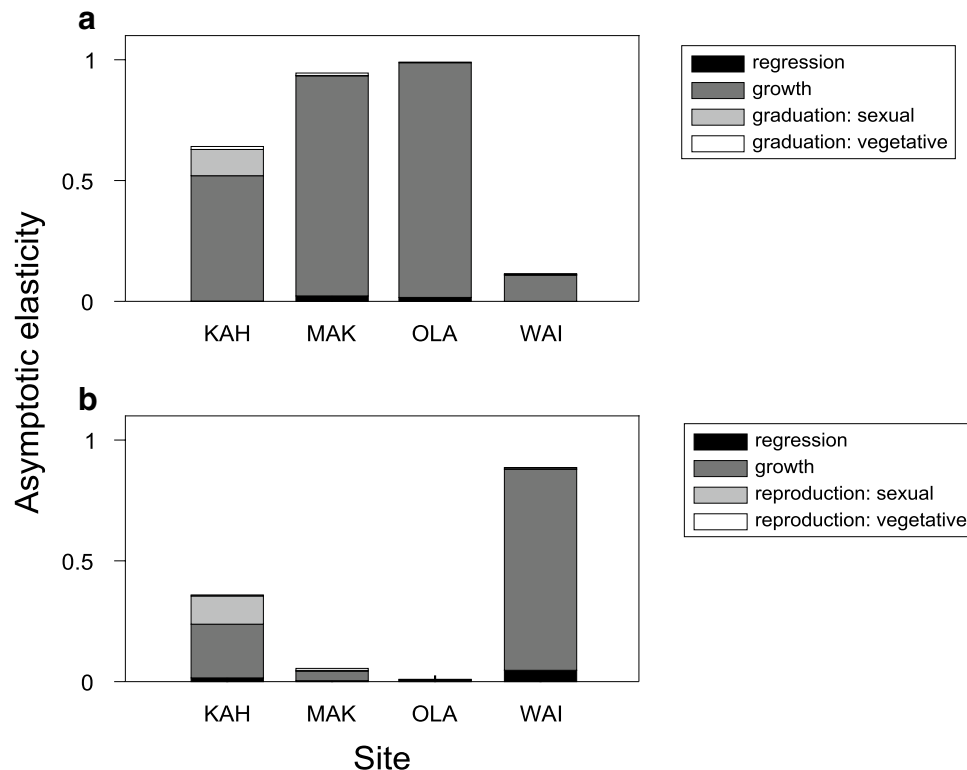


Fig. 5 Asymptotic elasticity summed by life history block of the matrix at four study sites, Kahauale‘a (KAH), Maka‘ala (MAK), ‘Ola‘a (OLA) and Waiākea (WAI). Note that for a given site, the column sum across panels (a) and (b), will include all eight blocks of the matrix and thus will be equal to 1. **a** For stems with $DBH < 0.5$ cm, the life history blocks of the matrix include regression, growth, “graduation” of stems originating as sexual offspring and “gradu-

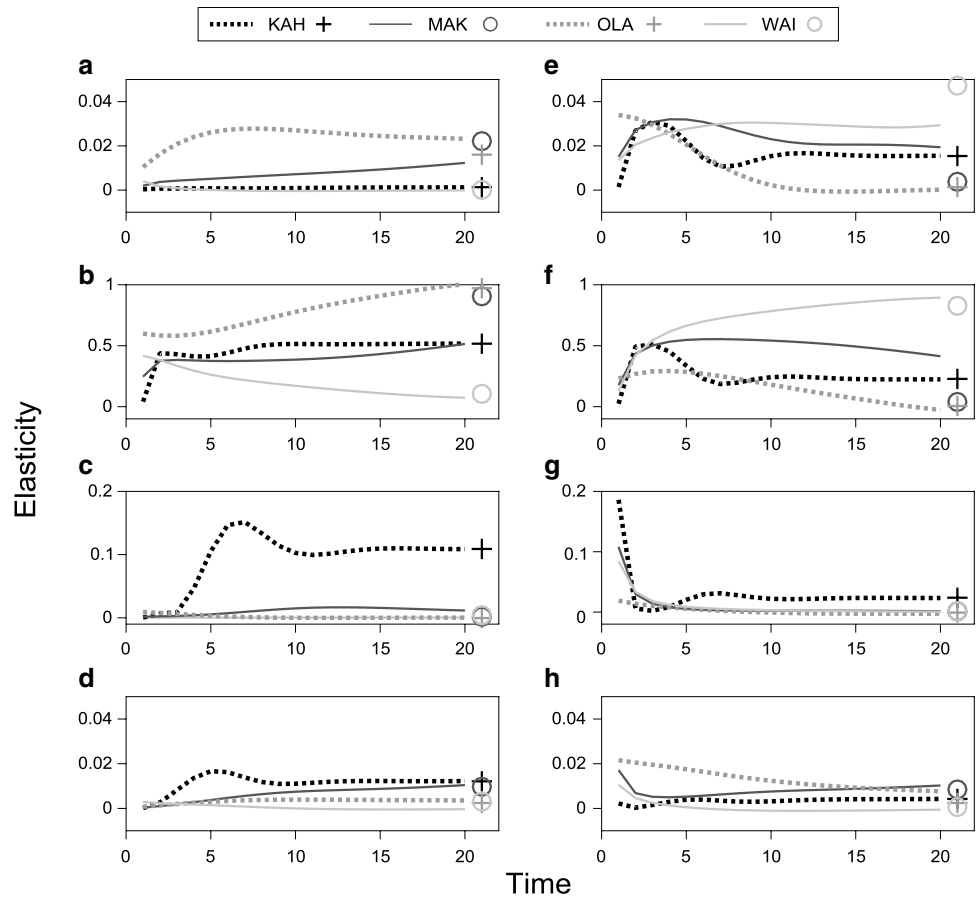
ation” of stems originating as vegetative offspring, where “graduation” refers to stems growing sufficiently large ($DBH \geq 0.5$ cm) to be counted in the continuous domain at the next time step. **b** For stems with $DBH \geq 0.5$ cm the life history blocks of the matrix include regression, growth, sexual reproduction, and vegetative reproduction, where reproduction refers to the production of offspring to be counted in the discrete domain at the next time step

from seeds into the large domain were also important, contributing 11.7 and 10.9%, respectively, to total elasticity (Fig. 5, left hand column).

Elasticity of transient population growth rate to proportional perturbations in different blocks of the matrix varied among populations similarly to asymptotic elasticity (Fig. 6). For example, the population at ‘Ola‘a had very high elasticity for perturbations to growth of small stems (Fig. 6b), while the population at Waiākea had the highest elasticity for perturbations to growth of large stems (Fig. 6f) and the population at Kahauale‘a had higher elasticities than the other sites for sexual reproduction (Fig. 6g) and graduation of small stems that originated from seeds (Fig. 6c). Patterns in the transient dynamics that were not found in the asymptotic dynamics included the following: ‘Ola‘a had higher elasticity for perturbation to regression of small stems than any other site (Fig. 6a), while Waiākea had higher elasticity for perturbations to regression of large stems than any other site at later times, but not initially (Fig. 6e) and Kahauale‘a had higher elasticities than the other sites for graduation of small stems that originated vegetatively (Fig. 6d).

Populations had different rhythms and amplitudes of change across time; the timing of the peaks and valleys varied across life history blocks even for a given site (Fig. 6). In all blocks of the matrix for both large and small stems, there were changes over time in the relative order of the elasticity for one population vs another. At all sites, the elasticity to sexual reproduction was at a maximum at the first time $t = 1$ (Fig. 6g), with relatively little change over time at ‘Ola‘a compared to the other sites. The most conspicuous oscillations were projected for Kahauale‘a where the peak elasticity to graduation of stems that originated vegetatively was at $t = 5$ (Fig. 6d), while the peak elasticity to graduation of stems that originated from seeds was a bit later (Fig. 6c). For ‘Ola‘a, elasticity of all life history blocks of large stems declined with time (Fig. 6e–h), while elasticity to growth of small stems increased over time (Fig. 6b). For Maka‘ala, there appears to be subtle projected attenuated oscillations, with elasticity to growth (Fig. 6f) and regression (Fig. 6e) of large stems first rising and then falling over time. Also elasticity levels at $t = 20$ for this site are often far from the asymptotic (Fig. 6a, b, e, f), suggesting a longer transient

Fig. 6 Transient elasticities (first 20 time steps) summed by life history block of the matrix at four study sites, Kahauale‘a (KAH), Maka‘ala (MAK), ‘Ola‘a (OLA) and Waiākea Forest Reserve (WAI). The value for the asymptotic elasticity of each site is included for reference, demarcated by a plus sign at the far right of each line. The elasticities for stems with DBH < 0.5 cm are in **(a)** regression, **(b)** growth, **(c)** graduation of stems originating as sexual offspring, and **(d)** graduation of stems originating as vegetative offspring; for those with DBH ≥ 0.5 cm elasticities are in **(e)** regression, **(f)** growth, **(g)** sexual reproduction, and **(h)** vegetative reproduction. The y-axes of the panels are scaled to give maximum resolution to any site differences within a life history block rather than scaled to illustrate differences among the life history blocks



period for this population. For Waiākea, elasticity to growth and regression of large stems (Fig. 6e, f) increased with time, while elasticity to both vegetative and sexual reproduction (Fig. 6g, h) declined with time.

Discussion

Variability in demography among replicate populations

Having focused on variability among populations that were initially selected for their overall similarity, not for their differences, we found substantial dynamically relevant variation. The conclusion is that managers should expect substantial site-to-site variability in the near- and long- term population dynamics of invasive species and in the sensitivity of annual per capita population growth rate to perturbations of different aspects of life history. Our sampling regime does not allow us to determine whether the variation we uncovered is associated with any causal factor (environmental, genetic, introduction history, etc.). Our study species, strawberry guava, has invaded a wide array of habitats in Hawai‘i from sea level to 4800 m with moderate to high

rainfall. Demographic variation associated with such environmental gradients is likely to be even greater.

Populations were projected to increase at all the study sites (Fig. 2a), but at different rates (Fig. 2b, c). The population Kahauale‘a, which was projected to have the highest per capita population growth rate in both the near- (Fig. 2b) and long- (Fig. 2c) term would require aggressive intervention to control whereas the population at Waiākea (Fig. 2a, b) would require less intervention. All the study populations were projected to change in structure during the transient phase (Fig. 3), even in the absence of any management. For example, juveniles were projected to make up an ever-increasing portion of the population. Focusing on the two sites of most (Kahauale‘a) and least (Waiākea) concern to managers, we note that the relative proportion of juveniles that originate from sexually produced seeds was projected to increase dramatically over the transient phase (Fig. 3b compared to Fig. 3a). Meanwhile the relative proportion of the “non-juvenile” population that are in the 100 largest DBH classes (which are the size classes that have midpoints spanning the range from 9.84 to 19.04 cm) was projected to remain very low at Kahauale‘a, while increasing noticeably at Waiākea (Fig. 3d compared to Fig. 3b). These projected transient changes in structure at each site should be

considered a null hypothesis for evaluating any changes in structure that might be observed following the application of a management treatment.

Variability in key parameters of transient dynamics among replicate populations

There was marked variability among replicate populations in all three parameters that characterize transient dynamics. Taking the three metrics together, we can say that the transient effects are strongest at one of our sites Waiākea compared to the others; despite that we will not see large oscillations there in our 20 time-step projection. A general result is that there is variability among seemingly replicate populations in the relative importance of the transient dynamics.

When the asymptotic structure is reached $\alpha(t) = 1$. Comparing the trajectory of $\alpha(t)$ among populations allows us to evaluate the consequences of ignoring transient dynamics and just focusing on asymptotic dynamics. Our results indicate that the peril of ignoring transient dynamics varies among populations. Only one of our study populations (Kahauale‘a) was projected to attain $\alpha(t) = 1$ during the first 20 time steps; it was projected to cross that threshold for the first time within just a few time steps, then cycle around it with damped oscillations, converging within 5–10 time steps (Fig. 4b). The population for which $\alpha(20)$ was projected to be farthest away from 1 was Waiākea (Fig. 4a). This comparison implies that ignoring transient dynamics at Kahauale‘a (where their effects are projected to disappear within 5–10 time steps) would be less of a mistake than ignoring them at Waiākea (where their effects are projected to persist).

We reiterate the point emphasized by Maron et al. (2010) that the difference between initial and the asymptotic structures, particularly which stages are over- or under-represented in the initial distribution, is what determines the magnitude and length of the transient dynamics. We suggest, as they did, that researchers need a targeted protocol focused on obtaining a good estimate of initial structure. The ideal sampling regime for capturing size-specific rates of survival, growth and reproduction differs from the ideal sampling regime to determine population structure. The former would stratify sampling by plant size, while the latter would stratify by spatial variation. In situations where quantifying the existing stage structure of a population is difficult (for example in some conservation contexts), Townley et al. (2007) and Stott et al. (2010) outline a technique for calculating the outer bounds of transient dynamics without the need to know initial population structure. Their protocol does not lend itself to addressing the near-term effects of management decisions such as the projected near-term impact of introducing a bio-control agent. Our results suggest it would be ideal to have a good estimate of population

structure of the target *just prior* to the implementation of any new protocol.

The damping ratio ρ does not depend upon initial structure. It is $\ll 1$ when the subdominant eigenvalue has a much lower magnitude than the dominant, and conversely it is approximately 1 when the subdominant is nearly co-equal to the dominant. In the former case, convergence to asymptotic dynamics is very rapid and the transients can likely be ignored. Although none of our study populations had $\rho \ll 1$, there was substantial variation among them, lowest at Kahauale‘a and highest at Waiākea (Fig. 4c). The damping ratio is often used to address the issue of the time it will take for the dominant to be a *particular*-fold more important than the subdominant? For example, how much time it would take for the dominant to be two-fold more influential is given by $\tau = -\log(2)/\log(\rho)$. Performing this calculation, we found that it is projected to take 2.9, 4.2, 9.2 and 91.6 years for the dominant to be twice as influential as the subdominant at Kahauale‘a, ‘Ōla‘a, Maka‘ala and Waiākea, respectively. Once again, we see evidence that the influence of transient dynamics is expected to persist much longer at Waiākea than at the other sites. These results further support the notion that ignoring transient dynamics at some sites would be worse (in the sense of missing what is likely to happen) than ignoring them at other sites.

The number of time steps needed to complete one oscillation in the complex plane μ is another metric that does not depend upon initial structure. The background for this metric is that subdominant eigenvalues can be complex numbers that have a real and an imaginary component. A complex number describes a point in the complex plane and as such it can be expressed by polar coordinates as an angle and a length. Expressing the angle θ in degrees and recalling that one complete oscillation is 360° , $\mu = 360/\theta$. For example when $\theta = 90$, $\mu = 4$ time steps. The narrower the angle, the more time steps it will take for a complete oscillation. Only one of our sites Waiākea had a population projection matrix with a complex subdominant eigenvalue. Its angle was very narrow such that 150 time steps would be required for a complete oscillation, which is a very slow oscillation. This means we are unlikely to view the oscillatory behavior in a 10 or 20 time-step projection.

Transient dynamics vs temporal variability in demographic rates

Transient analysis looks at changes over time of population dynamics in the absence of environmental change over time; the same matrix is used to project the population during the transient and asymptotic phases. A quite distinct scenario is temporal variability in demographic rates (stage-specific growth, survival and reproduction) themselves, i.e., the matrix itself changes over time. Analysis of long run

variation of this kind is addressed by tools that focus on sequences of matrices; including random matrix products for stochastic sequences and other approaches for deterministic sequences. In either case the (long run) cumulative per capita population growth rate over time and its geometric root are key analytic quantities (e.g., Tuljapurkar et al. 2003; Morris et al. 2006). Transient dynamics are at work here as well, since no single matrix stays around long enough for its asymptotic dynamics to be realized. Such concepts, while not the focus of this paper, could also be relevant to analyzing the effects of management protocols. For example, after a bio-control agent is introduced, eventually it is expected that a dynamic equilibrium in the species interaction (or at least the long-term persistence of both species) would emerge and demographic rates of both could exhibit some predictable interactive patterns over time (Buckley et al. 2005).

Linking evolutionary ecology to demography in context of transient elasticity

We can make use of the rich array of results above to address the question of the potential for variability among populations in their response to targeted management protocols like the introduction of a bio-control. The same approach applies to addressing the question of selection on particular traits of the invasive species. The first step is to identify which of the different components of the life history of the invasive species are likely to experience the *direct* effects of the management protocol or be directly influenced by the trait. The second step is to consider how sensitive fitness is to that effect at each time step; that is, to examine the transient elasticity of population growth rate to that effect. By *direct* effects, in the context of our model, we mean a measurable effect on a particular matrix element or group of elements. For example, Maron et al. (2010) employed transient and asymptotic elasticity analysis for the interaction of a potential bio-control insect with a perennial herb *Cynoglossum officinale* invasive in North America. In that case, experimental data had established that the principal direct effect of the insect was to lower per capita seed production of the plant by 30%. Thus the elasticity analysis focused on seed production; it revealed that reproduction by particular stages were more influential than others. The transient elasticities for those particular stages' reproduction provided insight to the timing of the maximal effect of the insect on the plant during the transient period (which turned out to be at $t = 1$). Transient elasticities indicate temporal variability in selection pressures. It is quite possible that a given management protocol could have a large impact on near-term dynamics (defined as the first few years), even if it would not be important to long-term dynamics projected by the matrix, or *vice versa*. Such differences should show

up as a difference between transient and asymptotic elasticity of annual per capita population growth rate to perturbations of those particular demographic rates (i.e., matrix elements) that are most directly affected by the protocol.

The ecological context of a bio-control-host interaction in a non-native region can be thought of as a novel interaction with new evolutionary dynamics, despite a previous evolutionary history on another continent. A host that has established itself as an invasive pest in a non-native region has been free of selection by its native enemies for several generations. Its demographic rates and traits related to defense are likely distinct from what they were in the native range as a result. Also, in the native range, the enemy itself was subject to competition and predation and it likely had multiple hosts, but when the enemy is intentionally introduced into a non-native region as a bio-control agent its competitors, predators and alternate hosts are not introduced with it and its demographic rates are also likely quite distinct from what they were in the native range (Pearse and Altermatt 2013; Saul and Jeschke 2015). We can consider the time of introduction as a starting time for the interaction in its novel context; neither species is expected to be at its stable stage distribution. Thus transient dynamics and their analysis are relevant to the evolutionary ecology of the interaction (McMahon and Metcalf 2008; Maron et al. 2010) in the near term.

Experimental work on the relative preferences and effects of a bio-control on target individuals of different developmental stages and/or microhabitats could yield useful insights. A planned bio-control agent on strawberry guava, *T. ovatus*, is a scale insect that induces gall formation. It is expected to broadly reduce both growth and reproduction. What if *T. ovatus*, for example, prefers to be in the canopy and thus to feed on plants ≥ 0.5 cm DBH rather than in the understory where it would feed on small plants (< 0.5 cm DBH)? Then, focusing on elasticity for the block of the matrix that includes growth of the large stems, we note that asymptotic population growth rate is very sensitive to perturbations of growth of large stems at Waiākea and very insensitive to perturbations of growth of large stems at 'Ōla'a, with the other populations intermediate (Fig. 5b). These results indicate that *T. ovatus*, for example, would be more successful in controlling the population of strawberry guava at Waiākea compared to the other sites in the long run. What about in the near term? Perturbation of the growth of large stems has relatively little impact on population growth and there is little difference among the sites at the beginning of the transient phase, but the differences among sites increases as time goes by. By $t = 5$, Waiākea emerged as and remained as the site with the highest elasticity. In fact elasticity for this block increases throughout the transient phase for this site, even though in the first year, it was not the site with the highest elasticity for growth of large stems.

A cautionary lesson with management implications under this scenario would be that even though early on a management protocol may have similar (albeit low) impacts on population growth of several local populations, it may soon show quite different impacts at different populations for no other reason than that of distinct transient dynamics among populations. Whichever type of life history transition is affected by any management protocol, the initial differences in its effects among the populations will not be what we see at other points in time or in the asymptotic projection. For all the life history blocks, the relative order of the elasticity for one population vs another may well change during the transient phase. This means that even if it is most effective at one site compared to other sites in the first few years, it could well be more effective at different site a few years later, even in the absence of changes in demographic rates across time.

Acknowledgements We thank Cheyenne Perry USDA FS; Erin Raboin USDA FS; Nancy Chaney USDA FS; University of Hawai‘i-Hilo student volunteers and assistants for help for help with field measurements and data management. We thank the Division of Forestry and Wildlife, Hawai‘i Department of Land & Natural Resources (DLNR) for supporting establishment of study plots on Forest and Natural Area Reserves and USDA Forest Service and the DLNR Hawai‘i Watershed Partnership Program for funding.

Appendix

In this paper we express the population dynamics of a structured population as a trajectory over time (see Eq. 3), that has both transient and asymptotic phases. In the main body of the paper we are mainly focused on the transient phase. In this “Appendix”, we provide the mathematical underpinnings of both phases and we describe the key parameters of asymptotic dynamics to set the stage for their transient analogues. As time proceeds, the total number of individuals $N(t)$ changes as does their distribution into categories, $\mathbf{n}(t)$. Mathematically, the underlying dynamics can be expressed as combinations of all the eigenvalues (speeds) and eigenvectors (directions) of the matrix \mathbf{A} . For a matrix of dimension S , there are S eigenvalues λ_i , each with corresponding right and left eigenvectors, \mathbf{u}_i and \mathbf{v}_i where i goes from 1 to S . All the speeds and directions contribute to the population at each time step,

$$\mathbf{n}(t) = \sum_{i=1}^{i=S} c_i \lambda_i^t \mathbf{u}_i, \quad (3)$$

where each term in the summation corresponds to one of the directions, each c_i is a weighting of that direction in relation to the initial vector of the population and each λ_i is raised to the t th power. In general the eigenvalues can be positive or negative, real or complex (complex conjugate

pairs). Of particular interest is what happens to contributions from these different kinds of eigenvalues (real, complex, negative, positive) as they are raised to successively higher powers. If we have a matrix that is non-negative and mathematically irreducible and primitive (most population projection matrices in practice do have these features), there will be one real, positive eigenvalue that is larger in magnitude than any other (Perron-Frobenius theorem, see Caswell 2001, Chap. 4). The influence of this particular eigenvalue λ_{dom} and its associated eigenvectors (\mathbf{u}_{dom} and \mathbf{v}_{dom}) will come to dominate population dynamics given sufficient time. Thus, as time goes to infinity (and often much, much sooner), the population reaches a characteristic shape corresponding to the right eigenvector associated with the dominant eigenvalue. Asymptotically, the distribution of the population attains and maintains the shape seen in the dominant right eigenvector \mathbf{u}_{dom} , known as the *stable stage distribution* (Caswell 2001, Chap. 4). It is independent of the shape of the initial population vector. Concomitantly, the population attains and maintains a particular rate of per capita growth (or shrinking) time after time, the rate given by the dominant eigenvalue. The dominant left eigenvector \mathbf{v}_{dom} provides a measure of the reproductive value of individuals of different sizes, addressing the question of the relative important of each size as a seed for future population. Analyses of population projection matrix models often focus on asymptotic dynamics: the dominant eigenvalue, its associated left and right eigenvectors, and its sensitivity and elasticity (proportional sensitivity) to perturbations. Since, each life cycle event corresponds to one element a_{ij} of the matrix \mathbf{A} , biologically, sensitivity addresses the issue of how very small changes (perturbations) in life cycle events would impact the asymptotic population growth rate λ_{dom} . To facilitate the calculation of sensitivities, we followed the common practice of normalizing the right dominant eigenvector \mathbf{u}_{dom} to sum to 1 and then normalizing the left dominant eigenvector \mathbf{v}_{dom} such that the scalar product (the sum of the element-wise products) of the two vectors equals 1 (as in Caswell 2001, Chap. 4). When left and right eigenvectors are normalized this way, each entry in the sensitivity matrix is readily calculated as a product of the j th element of the right dominant eigenvector with the i th element of the left dominant eigenvector,

$$s_{ij} = u_{dom}(j) v_{dom}(i). \quad (5)$$

Each entry in the elasticity matrix is readily calculated as a product of the sensitivity with the original matrix entry divided by the dominant eigenvalue,

$$e_{ij} = s_{ij} a_{ij} / \lambda_{dom}. \quad (6)$$

Asymptotic elasticities are positive and sum to 1; in this sense they represent proportional contributions.

References

- Asner GP, Hughes RF, Varga TA, Knapp DE, Kennedy-Bowdoin T (2009) Environmental and biotic controls over aboveground biomass throughout a tropical rain forest. *Ecosystems* 12:261–278
- Buckley YM, Rees M, Sheppard AW, Smyth MJ (2005) Stable coexistence of an invasive plant and biocontrol agent: a parameterized coupled plant-herbivore model. *J Appl Ecol* 42:70–79
- Caswell H (2001) *Matrix population models: construction, analysis, and interpretation*. Sinauer, Sunderland
- Caswell H (2007) Sensitivity analysis of transient population dynamics. *Ecol Lett* 10:1–15
- Easterling MR, Ellner SP, Dixon PM (2000) Size-specific sensitivity: applying a new structured population model. *Ecology* 81:694–708
- Ellner SP, Rees M (2006) Integral projection models for species with complex demography. *Am Nat* 167:410–428
- Fox GA, Gurevitch J (2000) Population numbers count: tools for near-term demographic analysis. *Am Nat* 156:242–256
- Gagne WC, Cuddihy LW (1999) Vegetation. In: Wagner WL, Herbst DR, Sohmer SH (eds) *Manual of the flowering plants of Hawai'i*. Bishop Museum Special Publication 87. Univ. Hawai'i and Bishop Museum Press, Honolulu, pp 45–114
- Gaoue O (2016) Transient dynamics reveal the importance of early life survival to the response of a tropical tree to harvest. *J Appl Ecol* 53:112–119
- Giambelluca TW, Schroeder TA (1998) Climate. In: Juvik SP, Juvik JO (eds) *Atlas of Hawai'i*. Univ. Hawai'i Press, Honolulu, pp 49–59
- Giambelluca TW, Nullet MA, Schroeder TA (1986) *Rainfall atlas of Hawai'i*. R76. Dept. of Land and Natural Resources. Div. of Water and Land Development, Honolulu
- Haridas CV, Tuljapurkar S (2007) Time, transients and elasticity. *Ecol Lett* 10:1143–1153
- Horvitz CC, Pascarella JB, McMan S, Freedman A, Hofstetter RH (1998) Functional roles of invasive non-indigenous plants in hurricane-affected subtropical hardwood forests. *Ecol Appl* 8:947–974
- Iles DT, Salguero-Gómez R, Adler PB, Koons DN (2016) Linking transient dynamics and life history to biological invasion success. *J Ecol* 104:399–408
- Keyfitz N (1968) *Introduction to the mathematics of population*. Addison-Wesley, Reading
- Koons DN, Grand JB, Zinner B, Rockwell RF (2005) Transient population dynamics: relations to life history and initial population state. *Ecol Model* 185:283–297
- Maron JL, Horvitz CC, Williams JL (2010) Using experiments, demography and population models to estimate interaction strength based on transient and asymptotic dynamics. *J Ecol* 98:290–301
- McMahon SM, Metcalf CJE (2008) Transient sensitivities of non-indigenous shrub species indicate complicated invasion dynamics. *Biol Invasions* 10:833–846
- Morris WF, Tuljapurkar S, Haridas CV, Menges ES, Horvitz CC, Pfister CA (2006) Sensitivity of the population growth rate to demographic variability within and between phases of the disturbance cycle. *Ecol Lett* 9:1331–1341
- Pearse IS, Altermatt F (2013) Predicting novel trophic interactions in a non-native world. *Ecol Lett* 16:1088–1094
- Saul WC, Jeschke JM (2015) Eco-evolutionary experience in novel species interactions. *Ecol Lett* 18:236–245
- State of Hawai'i, Department of Agriculture (2011) *Final environmental assessment: biocontrol of strawberry guava by its natural control agent for preservation of native forests in the Hawaiian Islands*. State of Hawai'i, Honolulu
- Stott I, Franco M, Carslake D, Townley S, Hodgson D (2010) Boom or bust? A meta-analysis of transient population dynamics in plants. *J Ecol* 98:302–311
- Takahashi M, Giambelluca TW, Mudd RG, DeLay JK, Nullet MA, Asner GP (2011) Rainfall partitioning and cloud water interception in native forest and invaded forest in Hawai'i Volcanoes National Park. *Hydrol Process* 25:448–464
- Townley S, Hodgson DJ (2008) Erratum et addendum: transient amplification and attenuation in stage-structured population dynamics. *J Appl Ecol* 45:1836–1839
- Townley S, Carslake D, Kellie-Smith O, McCarthy D, Hodgson DJ (2007) Predicting transient amplification in perturbed ecological systems. *J Appl Ecol* 44:1243–1251
- Tuljapurkar S, Horvitz CC, Pascarella J (2003) The many growth rates and elasticities of populations in random environments. *Am Nat* 162:489–502
- Uowolo AL, Denslow JS (2008) Characteristics of the *Psidium cattleianum* (Myrtaceae) seed bank in Hawaiian lowland wet forests. *Pac Sci* 62:129–135
- Vitorino MD, Pedrosa-Macedo JH, Smith CW (2000) The biology of *Tectococcus ovatus* Hampel (Heteroptera: Eriococcidae) and its potential as a biocontrol agent of *Psidium cattleianum* (Myrtaceae). In: Spencer NR (ed) *Proceedings of the X International Symposium on Biological Control of Weeds*, 4–14 July 1999. Montana State University, Bozeman, Montana, pp 651–657
- Wolfe EW, Morris J (1996) *Geologic map of the Island of Hawai'i*. Map 1-2524A. U. S. Department of the Interior, U. S. Geological Survey Miscellaneous Investigations Series, Washington, DC
- Zuidema PA, Jongejans E, Chien PD, During HJ, Schieving F (2010) Integral projection models for trees: a new parameterization method and a validation of model output. *J Ecol* 98:345–355